Heat pump assisted drying of flower bulbs

Wagenaar, S.; Infante Ferreira, C.A.

Publication date
2021

Document Version
Accepted author manuscript

Published in
Proceedings of the 13th IEA Heat Pump Conference (HPC2020)

Citation (APA)
Wagenaar, S., & Infante Ferreira, C. A. (2021). Heat pump assisted drying of flower bulbs. In *Proceedings of the 13th IEA Heat Pump Conference (HPC2020)* (pp. 1610-1620). IEA.

13th IEA Heat Pump Conference
April 26-29, 2021 Jeju, Korea

Heat pump assisted drying of flower bulbs

Sjors Wagenaar[ab], Carlos Infante Ferreira[a*]

[a]Delft University of Technology, Department Process & Energy, Leeghwaterstraat 39, 2628 CB Delft, The Netherlands
[b]Wagenaar Koeltechniek, Zaadmarkt 17, 1681 PD Zwaagdijk-Oost, The Netherlands

Abstract

Within the agriculture sector, drying of food and flowering products is a required production step. Most companies use hot air dryers where the heat is obtained by combustion of natural gas. This paper proposes a heat pump assisted drying system as an alternative. Flower bulb carrying boxes containing just harvested products have been approximated as packed beds filled with spherical products. A heat pump is proposed which includes a cross flow heat exchanger and allows for recirculation of the drying air while maintaining its operating temperature and humidity at optimal conditions to guarantee the required drying rate while preventing damage of the product. Simulink is used to optimize the operating conditions of the system guaranteeing both the product quality and a low energy consumption. The heat pump has been sized to dry 10 flower bulb carrying boxes of about 800 kg each in 24 hours. The performance of the heat pump (170 kWh/day renewable electricity) is compared to the performance of conventional fossil fuel based drying systems (350 kWh/day fossil fuel). Understanding heat and mass transfer mechanisms during drying allows optimization of the heat pump design.

Keywords: heat pump, drying of horticulture products, moisture removal, experimental drying rates;

1. Introduction

1.1. Energy needs in field horticulture

Drying is an energy intensive process. It accounts for 10 to 20% of the total consumption of energy by industry in most developed countries [7]. Drying of agricultural products is commonly accomplished using hot air convective drying, where air is preheated by a gas burner or indirectly by a gas boiler. The Paris agreement from 2015 imposes the banning of fossil fuels as heat sources for drying processes. Heat pumps are currently the most appropriate technique to replace gas boilers. Heat pumps can both be used for heating and dehumidification purposes making its users less dependent on weather conditions, lowering the energy consumption and guaranteeing a constant high product quality. When renewable electricity is used to drive the heat pumps, its operation is fully independent of fossil fuels.

The agricultural sector can be divided in field horticulture (production and processing of food and flowers), greenhouse horticulture, animal farms, wood processing and fishing. These sectors, in the Netherlands, consume 140 PJ of primary energy corresponding to CO_2 emissions of 7.3 Mton. The strategy of the Dutch government [4] to fulfill to the Paris agreement by 2030 imposes a CO_2 emission reduction of 40% for the agricultural sector. According to Wildschut [18] the field production and processing of flowers and flower bulbs is responsible for about 5 PJ of primary energy. It is also expected that this sub-sector contributes to the CO_2 emission reduction with 40% . The sector has signed an agreement with the government that by 2023 16% of the energy use will come from renewable sources [18]. Implementation of heat pumps for drying needs in the sector making use of renewable energy will give significant contributions to these goals.

Nomenclature

* Corresponding author. Tel.: ++31-15-278-4894.
E-mail address: c.a.infanteferreira@tudelft.nl.

Roman characters			*Greek characters*		
A	Area	-	α	Heat transfer coeff.	$W/m^{-2}K^{-1}$
a_w	Water activity	-	Δh_{fg}	Evaporation heat	$kJkg^{-1}$
COP	Coefficient of performance	-	ε	Void fraction	-
c_p	Specific heat	$kJkg^{-1}K^{-1}$	ε_{CFHE}	Effectiveness CFHE	-
D	Diffusivity	m^2s^{-1}	λ	Thermal conductivity	$Wm^{-1}K^{-1}$
d_{bulb}	Bulb diameter	m	μ	Viscosity	Pa s
G	Mass flux	$kgs^{-1}m^{-2}$	ρ	Density	kgm^{-3}
k	Mass transfer coefficient	ms^{-1}	ω	Humidity ratio	$kg_{H2O}kg_a^{-1}$
L	Length	m			
$\dot{m}$	Mass flow	kgs^{-1}	*Subscripts*		
M	Molecular weight	$kgkmol^{-1}$	a	(Dry) air	
Nu	Nusselt number	-	c	Cross flow	
NTU	Number of transfer units	-	char	Characteristic	
p	Pressure	kPa	eq	Equilibrium	
Pr	Prandtl number	-	evap	Evaporation	
R	Universal gas constant	$kJkmol^{-1}K^{-1}$	G	Humid air side	
Re	Reynolds number	-	in	Inlet	
Sc	Schmidt number	-	int	Interface	
$SMER$	Spec. moisture extraction	$kgkWh^{-1}$	L	Liquid	
T	Temperature	K or ^oC	out	Outlet	
t	Time	s	sat	Saturated	
u	Velocity	ms^{-1}	v	Water vapor	
x	Moisture content bulb	$kg_{H2O}kg_{bulb}^{-1}$	w	Wetted effective	

1.2. Flower bulb processing

This study focus on flower bulbs. Flower bulbs generate heat by metabolism, absorb water and attract diseases when wet. After harvesting the flower bulbs need to be quickly dried to prevent that germs and fungi develop. Flower bulbs need to be conserved at specific temperature, water content and water activity. The water activity, a_w, gives the ratio between partial and saturated water vapor pressure at the surface of a product and is influenced by the temperature and humidity of the surrounding air. Also the concentration of CO_2 and ethylene around the flower bulbs need to be controlled to prevent health issues and contamination with external viruses. According to Wildschut et al. [19], a small amount of ventilation is, however, sufficient to prevent harmful concentrations. According to Rockland & Beuchat [14] a high water activity supports the growth of microorganisms, germination of spores and participation in several types of chemical reactions. Bacteria usually require at least a water activity of 0.91 and fungi of 0.60. So a flower bulb drying system should bring and maintain the water activity close to values just below 0.60. Every 1% of prevented product loss due to better conditioning of the drying and storage conditions results in savings of about € 16500. per year for the average farmer.

The transportation and storage of flower bulbs is usually realized in large cubic boxes of 0.8 to 1.2 m^3. These can be easily transported using forklift trucks. These boxes have a perforated bottom through which drying air can be circulated. Fig. 1 illustrates how the drying air flow from a central air treatment system can be distributed to a large number of these cubic boxes.

At the end boxes the forklift openings are blocked with foam creating a pressure rise which forces the air through the flower bulbs in the boxes. The return air is discarded or dehydrated and heated before being recirculated. The air temperature is maintained in the range 20 to 25 ^oC, depending on the cultivar. The average drying time of one batch is 24 to 36 hours and the amount of water that needs to be removed is around 50 kg per box [5].

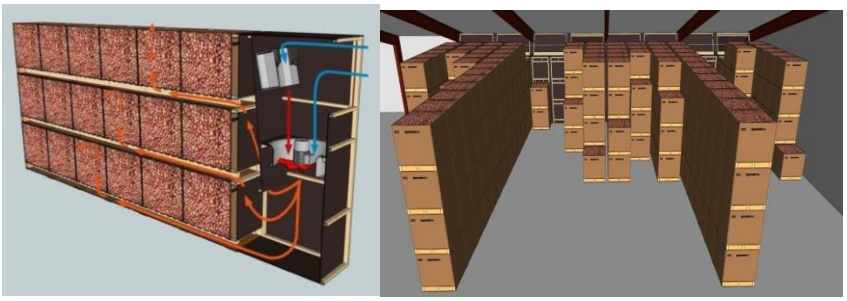

Fig. 1. Drying distribution arrangement for multiple flower bulb boxes.

1.3. Modeling of drying processes of agricultural products

Tzempelikos et al. [15] and Agrawal and Methekar [1] modeled the heat and mass transfer processes during drying of quince slices and pumpkin, respectively. Alnaimat et al. [2] and Li et al. [8] studied the heat and mass transfer processes in a structured packed bed column to determine temperature and humidity of air as it rises in countercurrent flow to cooled water. Minea [11] has reviewed the advances in heat pump drying technologies and its modeling approaches. Although these studies concern different drying processes, they have been used as the basis for the development of the flower bulb drying model introduced in this paper.

2. Drying of flower bulbs

The drying process starts by conditioning the air that is circulated along the bulbs to the required conditions (20 to 25 ºC; low humidity < 5 g/kg_{dry_air}). If possible heat recovery should be used. Then heat is transferred from the drying air to the surface of the bulbs while at the same time water evaporates from the surface of the bulb into the drying air flow. In this evaporation process surface water, or bounded water inside the product which has diffused into the surface, is removed from the bulb surface into the drying air flow. The resulting colder, humid air flows back into the conditioning system and is brought back to feed conditions. Mujumbar [12] distinguishes two drying rate regimes. In the begin of the process unbounded water is evaporated from the surface at a constant rate. When bounded water from the core of the bulb starts to be removed, at a critical moisture content of the bulb, the drying rate starts to decrease. This rate will then generally linearly decrease with the moisture content of the bulb until equilibrium is attained and the drying process stops.

2.1. Flower bulb properties

Bulbs are structured in multiple layers and have a strong solid surface which protects them against damage and diseases. Their structure is similar to the structure of onions and garlic which have been more frequently investigated. The effective moisture diffusivity of the flower bulbs, D, expressed in m^2/s has been assumed to be identical to the moisture diffusivity in onions as reported by Mujumbar [12] and is given in eq. 1 where the moisture content per kg bulb, x, is expressed in kg_{H2O}/kg_{bulb} and T, is the bulb temperature, in K.

$$D = \frac{1}{1+x} \cdot 1.45E-08 \cdot e^{\left[-\frac{70.2}{8314}\left(\frac{1}{T}-\frac{1}{333.15}\right)\right]} \quad (1)$$

Density, specific heat and thermal conductivity of onions reported by van Hiele et al. [16] have been assumed to apply for flower bulbs. Moisture content dependent values have been adopted from Kalbasi [6]. Its values are given in Table 1.

Table 1. Density, ρ, specific heat, c_p and thermal conductivity, λ of flower bulbs. x in kg_{H2O}/kg_{bulb} and T in K.

Properties of flower bulbs based on properties onions	$\rho_{product}$ (kgm^{-3})	$c_{p\_product}$ ($kJkg^{-1}K^{-1}$)	$\lambda_{product}$ ($Wm^{-1}K^{-1}$)	ρ_{bulk} (kgm^{-3})	c_{p_bulk} ($kJkg^{-1}K^{-1}$)	λ_{bulk} ($Wm^{-1}K^{-1}$)
Van Hiele et al. [16]	882	3.77	0.48	575	3.77	0.35
Kalbasi [6]		1.84+2.34*x	0.445+0.309*x-0.005*T			

In this study the water activity is obtained making use of the Chung-Pfost equation with the coefficients proposed for garlic bulbs by Madamba et al. [9]. The water activity is obtained using eq. 2 in which T is expressed in ºC.

$$a_w = e^{\left[-\frac{203.4}{T+76.5}\cdot e^{(-0.072\cdot x)}\right]} \tag{2}$$

The equilibrium moisture content of the bulbs can be related to the water activity. The Guggenheim-Anderson-de Boer equation predicts this relation over a wide range of water activity. For onions, Mujumbar [12] proposed eq. 3 with the parameters given in Table 2.

$$x_{eq} = \frac{b_0 \cdot b_1 \cdot b_2 \cdot a_w}{(1-b_1 \cdot a_w)\cdot(1-b_1 \cdot a_w + b_1 \cdot b_2 \cdot a_w)} \tag{3}$$

Table 2. Parameters proposed by Mujumbar [12] for the equilibrium moisture of onions in the Guggenheim-Anderson-de Boer equation. R in kJkmol^{-1}K^{-1} and T in K.

b_0	b_1	b_2	$b_{10}*10^5$	b_{11}	b_{20}	b_{21}
20.2	$b_{10}\cdot e^{\frac{b_{11}}{RT}}$	$b_{20}\cdot e^{\frac{b_{21}}{RT}}$	2.3	32.5	5.79	6.43

2.2. Modeling of drying process

The model has been developed for a single flower bulb carrying box. Fig. 2 illustrates how the box with coordinates *x, y* and *z* has been considered. The properties of flower bulbs and air flow are only changing in *z*-direction so that a control volume considers the whole *x-y* cross section of the box. The model is transient considering an one-dimensional step Δz in space and a time step Δt. The flow passage area of the box is constant along the height of the box and results in $z/\Delta z$ control volumes. Each control volume contains a volume fraction of flower bulbs, liquid and air. Multiplying each volume fraction with the corresponding material density results in the total mass in the control volume.

Fick's law allows for the determination of the mass transfer over the height of each control volume. This rate of mass transfer can be converted into the rate of humidity ratio change per control volume [17] as given in eq. 4.

$$\frac{d\omega}{dz} = \frac{k_G A_w}{G_a}\cdot\frac{M_v}{R}\left[\frac{p_v^{sat}(T_{\text{int}})}{T_{\text{int}}} - \frac{\omega}{0.622+\omega}\cdot\frac{p}{T_G}\right] \tag{4}$$

In this equation M_v is the molecular weight of the water vapor, R the universal gas constant, T_G (K) the air temperature, T_{int} (K) is the interface temperature (the flower bulb surface temperature), k_G (m/s) is the mass transfer coefficient, A_w (m^2/m^3) is the wetted effective surface area per unit volume. G_a is the mass flux of air through the cross flow area of the box, A_c, and p is the total system pressure.

The change in air temperature is obtained from the energy balance [17] and is given in eq. 5.

$$\frac{dT_a}{dz} = \frac{\frac{d\dot{m}_v}{dz}\cdot\Delta h_{fg} - \alpha\cdot(T_G - T_L)\cdot A_w\cdot A_c - \frac{d\dot{m}_v}{dz}\cdot(2501.1+1.8135\cdot T_{a\_in})}{\dot{m}_a\cdot c_{p\_a} + 1.8135\cdot\dot{m}_v + 1.8135\cdot\frac{d\dot{m}_v}{dz}} \tag{5}$$

where

$$\frac{d\dot{m}_v}{dz} = \frac{d\omega}{dz}\cdot\dot{m}_a \tag{6}$$

and T_L is the flower bulb surface temperature. The heat transfer coefficient between flower bulb surface and air, α, has been obtained from the correlation proposed in Mills [10] for spherical shaped packed beds.

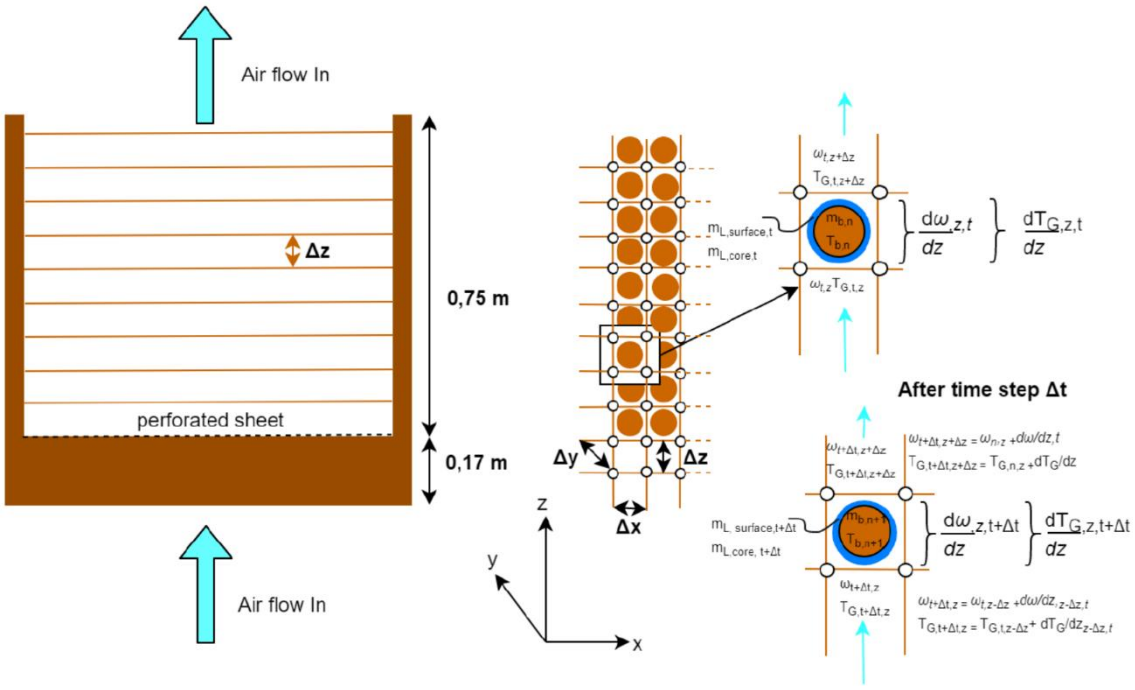

Fig. 2. Discretization of the flower bulb box considering it as a packed bed of flower bulbs.

$$\alpha = \frac{\lambda_a}{L_{char}} \cdot Nu = \frac{\lambda_a}{L_{char}} \cdot (0.5 \cdot \mathrm{Re}^{0.5} + 0.2 \cdot \mathrm{Re}^{0.67}) \cdot \mathrm{Pr}_a^{0.33} \tag{7}$$

With the characteristic length L_{char} obtained from eq. 8.

$$L_{char} = d_{bulb} \cdot \frac{\varepsilon}{1-\varepsilon} \tag{8}$$

With ε the void fraction of the packed flower bulb bed which was initially assumed to be 0.26 [3]. The Reynolds of the flow is calculated using eq. 9:

$$\mathrm{Re} = \frac{G_a \cdot L_{char}}{\mu_a} \tag{9}$$

The mass transfer coefficient is obtained making use of the Chilton-Colburn analogy.

$$k_G = \frac{\alpha}{\rho_a \cdot c_{p\_a}} \cdot \left(\frac{\mathrm{Pr}}{Sc}\right)^{0.67} \tag{10}$$

The wetted effective surface area per unit volume is obtained considering that the flower bulbs are spheres and taking the void fraction into account.

$$A_w = \frac{6}{d_{bulb}} \cdot (1-\varepsilon) \tag{11}$$

The pressure drop through the packed flower bulb bed has been predicted making use of the Ergun equation for packed beds, as proposed by Mills [10].

$$\frac{dp}{dz} = \frac{150 \cdot \mu_a \cdot u_{char}}{L_{char}^2} + \frac{1.75 \cdot \rho_a \cdot u_{char}^2}{L_{char}} \tag{12}$$

With the characteristic velocity obtained from eq. 13.

$$u_{char} = \frac{G_a}{\rho_a \cdot \varepsilon} \tag{13}$$

During the second drying regime mainly internal diffusion dominates the process. To take this into account the volume of the flower bulb has been discretized into several nodes between which diffusion is calculated. Details of the approach have been reported in Wagenaar [17].

3. Experimental data

During the summer of 2018 experimental data of the drying period have been collected at two different companies: Niels Kreuk BV and Gebr. Boon Hem BV. Data have been collected of temperature, relative humidity, total mass and pressure drop for batches of flower bulb boxes. Here only the data obtained at Niels Kreuk BV is discussed.

A schematic of the drying chamber and drying arrangement is shown in Fig. 3. This company makes use of a heat pump to dry its flower bulbs. In this arrangement dry air enters the flower bulb boxes from the top and the humid air leaves at the bottom. The air is then dried and heated by a heat pump. The figure shows the position of the boxes which have been measured.

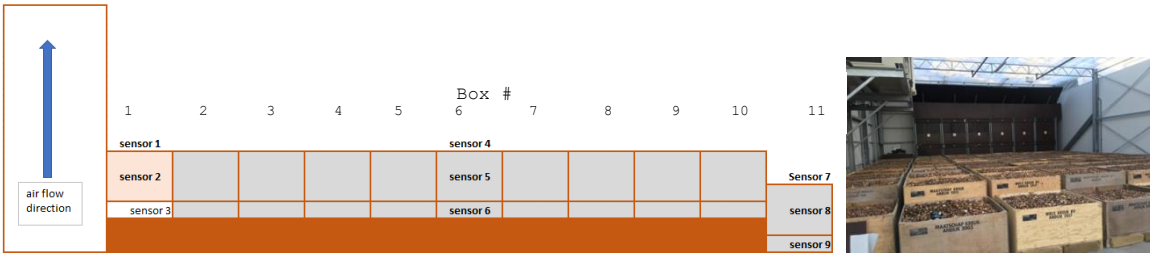

Fig. 3. Schematic of the heat pump based drying chamber of Niels Kreuk BV.

Table 3 shows the mass reduction of the different flower bulb boxes after 15 h and after 62 h of operation. The initial mass is the mass of the boxes just arriving from the field and before starting the drying operation.

Table 3. Mass reduction during the drying period of flower bulb boxes at Niels Kreuk BV. Data collected in July 2018.

	Initial mass [kg]	**Mass after 15 h [kg]**	**Reduction [kg]**	**Reduction [%]**	**Mass after 62 h [kg]**	**Reduction [kg]**	**Total Reduction [%]**	**Total mass removed [kg]**
Box 1	830	804	26	3.1	794	10	4.3	36
Box 6	790	772	18	2.3	762	10	3.5	28
Box 11	816	799	17	2.1	788	11	3.4	28

The table makes clear that the amount of moisture (and probably remaining soil) in each box is different so that in average the drying percentage is 4.1% but that the contents of some boxes dry 3.4% while of others dry up to 4.3%. The temperature and relative humidity have been measured by installing Lascar EL-USB-2 temperature and humidity data loggers in the different boxes. The temperature is measured with an accuracy of ± 0.5 K and the relative humidity with an accuracy of ± 2%. Fig. 3 shows that for some boxes the temperature and humidity change of the air flow as it passes the boxes have been measured. Fig. 4 illustrates how temperature and humidity change with time at inlet, halfway and at outlet of box 11. The air volume flow rate has been measured making use of an anemometer from Testo-air and mounting a plate with anemometer size perforations above the boxes. The measuring probe of Testo-air 435 has an accuracy of ± 0.1 m/s. The air volume flow through the boxes varies linearly with the position with the largest flow through box 1 (1600 m^3/h) and the lowest through box 11 (1200 m^3/h).

Fig. 4 makes clear that the control of the air inlet temperature and humidity was not able to maintain the air inlet conditions during the experimental period. In the first hour of operation, the air leaving the first half of the box was already saturated with water so that the relative humidity halfway the box is already identical to the relative humidity at the outlet of the box. It is only after about 20 minutes that the orange line starts decreasing. During some periods it is clear that the air inlet and outlet humidity did not change indicating that there was no humidity removal during these periods.

The pressure drop across the flower bulb box was 220 Pa for a volume flow rate of 1417 m^3/h and, respectively, 180 Pa and 100 Pa for volume flow rates of 1259 m^3/h and 917 m^3/h. These data have been used to calibrate the value of the void fraction. This was done by adjusting the value of the void fraction in eq. 13 until the result of eq. 12 corresponded with the experimental data. A value of 0.196 was derived for the void fraction which is slightly lower than the value proposed by Conway & Sloan [3] which was 0.26. A void fraction of 0.196 has been further used in the model.

The experimental wetted effective surface area per unit volume taking the eventual dirt in the void between the flower bulbs into account has also been derived from the experimental data. Since the rate of mass transfer is constant during the first hour of operation, A_w can be derived from eq. 4 when it is assumed that the bulb surface is at wet bulb conditions. From the experimental data, a value of 0.198 is calculated for A_w. This corresponds to assuming an average flower bulb diameter of 4.1 cm in eq. 11, what is quite reasonable.

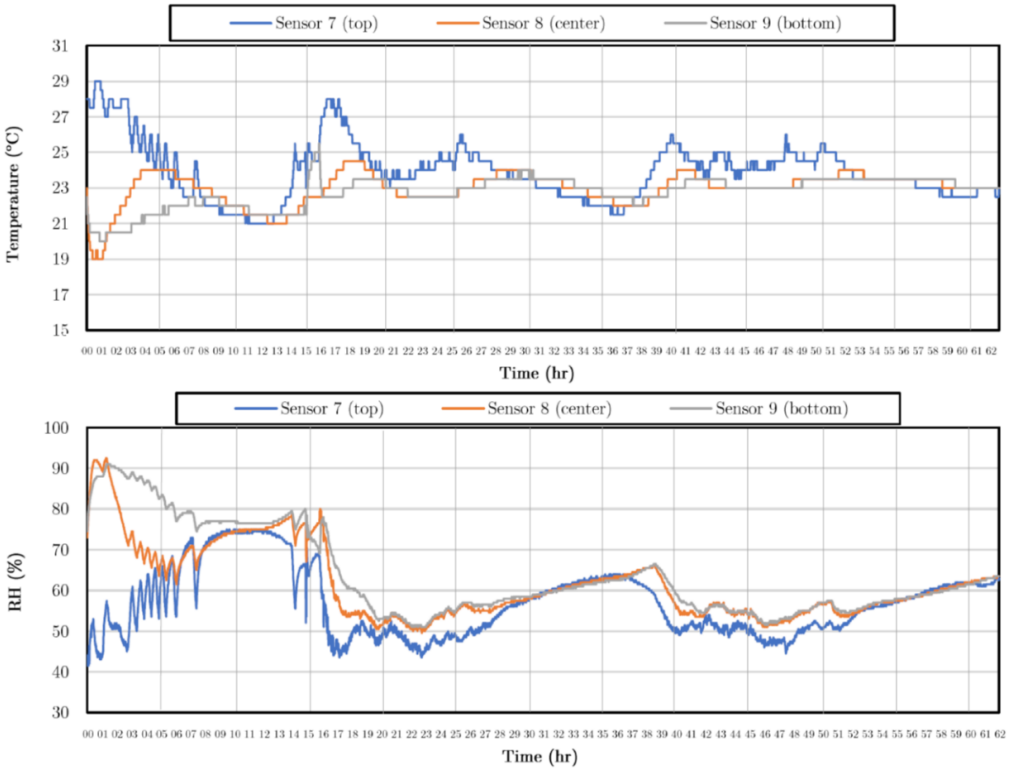

Fig. 4. Temperature (top) and relative humidity (bottom) of the air flow through the flower bulb box 11. Blue is inlet, orange halfway and grey is outlet. The time scale goes from 0 (start time) to 63 h (end of drying process).

4. Model validation

In Fig. 5 (left) the prediction of the model (light blue line) for the air outlet temperature is compared to the experimental outlet temperature (green line). The experimental inlet temperature (red line) is used as input for the model. The agreement is quite good. In Fig. 5 (right) the prediction of the model (light blue line) for the absolute humidity of the air at the outlet is compared to the experimental outlet absolute humidity (green line). The experimental inlet absolute humidity (red line) is used as input for the model. In the center the comparison of the relative humidity. The agreement is quite good.

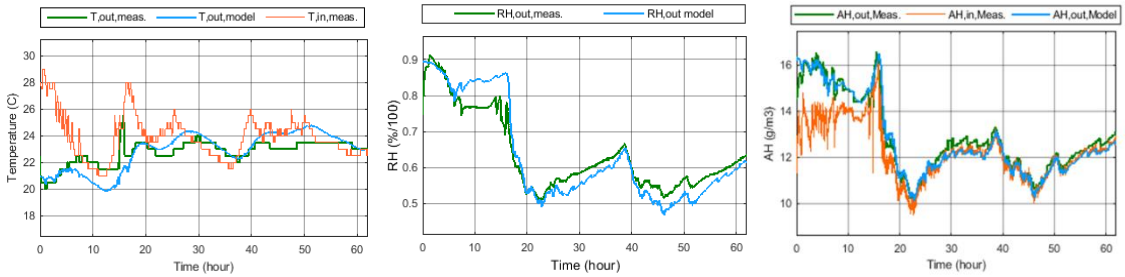

Fig. 5. Temperature (left) and absolute humidity (right) of the air flow through the flower bulb box 11. Red is inlet (experimental and also used as model input), light blue the outlet condition predicted by the model and green is experimental outlet. The time scale goes from 0 (start time) to 60 h (drying period).

Fig. 6 compares the progress of the drying process with the experimental data. The orange line gives the experimental data, the blue line gives the model prediction taking the flower bulb discretization into account and the purple line gives the model prediction based on the absolute humidity change and the air volume flow rate.

Using the flower bulb discretization to take the internal diffusion into account clearly improves the accuracy of the prediction. The model has been validated making use of the root mean square error method. Details of the validation have been reported by Wagenaar [17].

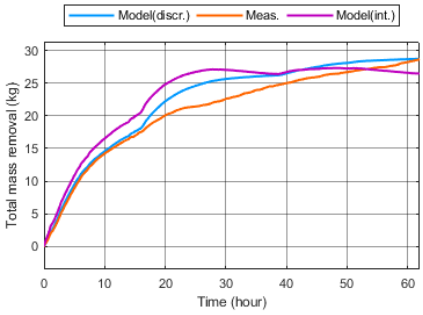

Fig. 6. Mass removed from box 11 as a function of time. The orange line shows the experimental data while the other two lines give the model prediction calculated in two different ways.

5. Heat pump dryer design

The flower bulb heat pump dryer proposed in this study is a typical vapor compression cycle assisted with a cross flow heat exchanger (CFHE). Its schematic and operating conditions are illustrated in Fig. 7. The system has been designed to remove the surface water of 10 flower bulb boxes in 8 h. Depending on the return temperature and humidity of the air after removing moisture from the boxes (state 1 in Fig. 7) the required evaporator capacity will vary from 40 to 60 kW. The heat pump should be able to remove 30 kg/h of water.

The heat pump has been modelled using simplified models for each component. Propane (R290) has been selected as the working fluid as it, as a natural refrigerant, has low environmental impact. A pressure ratio dependent isentropic efficiency has been adopted for the compressor, leading to efficiencies in the range 0.70 to 0.72 for the studied conditions. The evaporator and condenser dimensions and capacities have first been determined using the NTU-method. UA values of 3.55 and 3.20 kW/K have been obtained respectively for the evaporator and for the condenser. The heat exchanger effectiveness has then been used to predict the evaporating and condensing temperatures for different operating conditions, assuming these processes have infinite heat capacity. This is illustrated for the evaporator in eq. 14.

$$T_{evap} = \frac{T_{a\_out} - T_{a\_in} \cdot e^{-NTU}}{1 - e^{-NTU}} \tag{14}$$

The CFHE has also been modelled using the NTU-method as proposed by Ogulata & Doba [13] and its effectiveness is given in eq. 15.

$$\varepsilon_{CFHE} = 1 - 0.447 \cdot NTU^{-0.4} \tag{15}$$

The output temperature is then obtained from eq. 16 in which the indexes refer to states in Fig. 7.

$$T_2 = T_1 - 0.8 \cdot \varepsilon_{CFHE} \cdot (T_1 - T_3) \tag{16}$$

The 0.8 correction factor has been proposed by the CFHE manufacturer to take into account the condensation that takes place as the air passes the cold surface.

The heat pump dryer model has been implemented in Simulink. The schematic of the model is given in Fig. 8 and illustrates the links between the different components and the air flow conditions.

6. Heat pump dryer performance prediction

To prevent the air temperature to attain values above 35 ºC, what may damage the flower bulbs, the heat pump dryer is modelled with a constant air volume flow of 10000 m^3/h (1000 m^3/h per flower bulb box). Assuming that the air leaving the flower bulb boxes is almost saturated (95% relative humidity), the corresponding temperature and enthalpy at the evaporator outlet can be obtained. Then the required cooling

capacity can be determined and with it the required mass flow of refrigerant. The rotational speed of the compressor can then be adjusted to deliver the required cooling capacity.

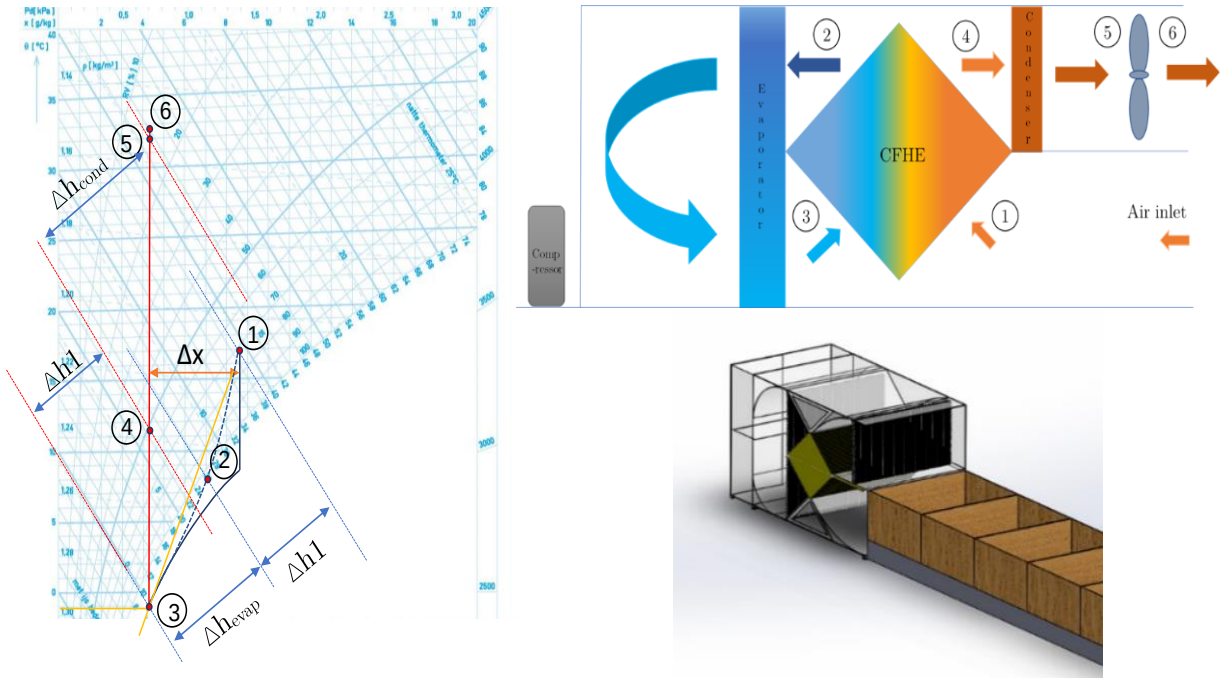

Fig. 7. The drying process in a Mollier diagram and schematic of the heat pump dryer. Between states 2 and 3 the air flow passes the evaporator of the heat pump and between 4 and 5 passes its condenser. State 1 is the return condition after removing moisture from the product. State 6 is the air condition as it enters the flower bulb boxes.

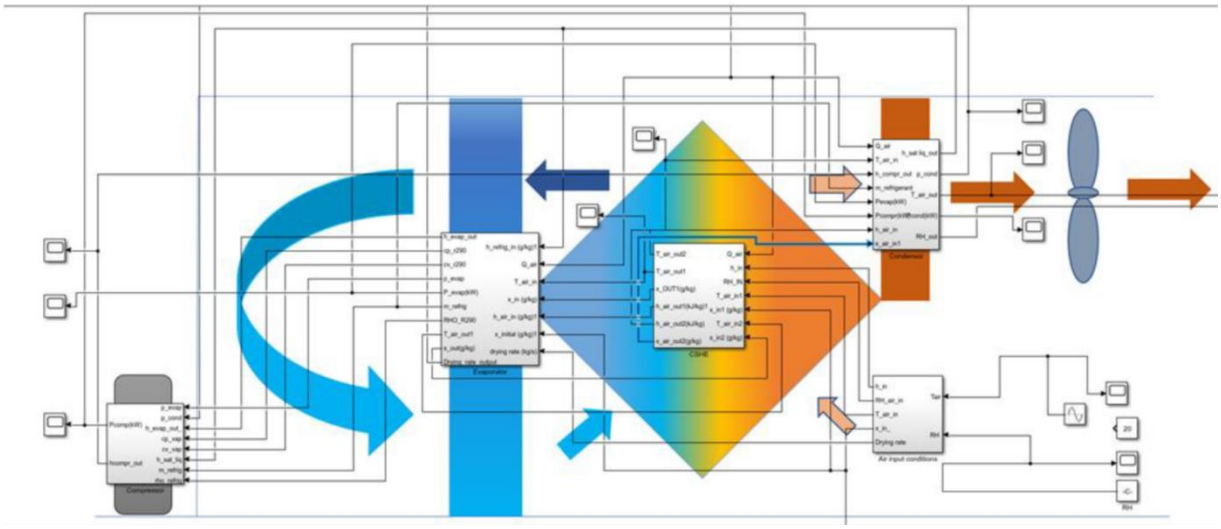

Fig. 8. Simulink model of the heat pump dryer showing the interaction between the different components of the system.

Fig. 9 shows, in the center, the predicted temperatures in the different positions of the heat pump system (the states are indicated in Fig. 7). The left hand side gives the temperature and relative humidity at the inlet and outlet of the heat pump dryer. The conditions of the air stream leaving the flower bulb carrying box (Fig. 5) are used as input for the heat pump dryer model. In the final stages of drying the humidity ratio remains practically unchanged between in- and outlet. Air enters at high temperature and low relative humidity and leaves at lower temperature and higher relative humidity. The right hand side of Fig. 9 gives the condensation and evaporation temperatures of the heat pump as predicted by the model. The evaporating temperature never goes below 0 ºC so that frost formation and associated problems are prevented. The condensation temperature reaches up to 40 ºC, a temperature about 7 K higher than the air outlet temperature and 15 K higher than the

air inlet temperature. The condensation temperature could be lowered by implementing a larger / external condenser to remove excess heat and with it the COP of the system would be improved.

The heat loads of the different components as predicted by the model and the corresponding coefficient of performance (*COP*) are given in Fig. 10 with left the heat loads, in the center the *COP* and the specific moisture extraction rate (*SMER*) expressed in kg/kWh and right the required mass flow of refrigerant. The refrigerant mass flow variation with time indicates that the compressor needs to operate between full-load and about 60% part-load. A range with very acceptable part-load performance.

Typical drying walls just increase the moisture removal capacity by preheating the drying air making use of hot water heat exchangers. The temperature of the drying air is conventionally increased with 4 K as the air passes these heat exchangers. Taking a boiler efficiency of 90% into account, heating 10000 m^3/h air requires a fuel heating power of 14.6 kW. This corresponds to a fossil fuel based energy consumption of 352 kWh per day. The left end side of Fig. 10 shows that during the first 24 hours the compressor of the heat pump (light blue line) consumes approximately 170 kWh renewable electricity. This is an energy consumption reduction of 57%. A CO_2 emission reduction will only be attained if the compressor is driven by renewable electricity. With an average energy conversion efficiency of 0.42 in the Dutch fossil fuel driven power stations, using electricity generated by these power stations will result in approximately the same CO_2 emissions.

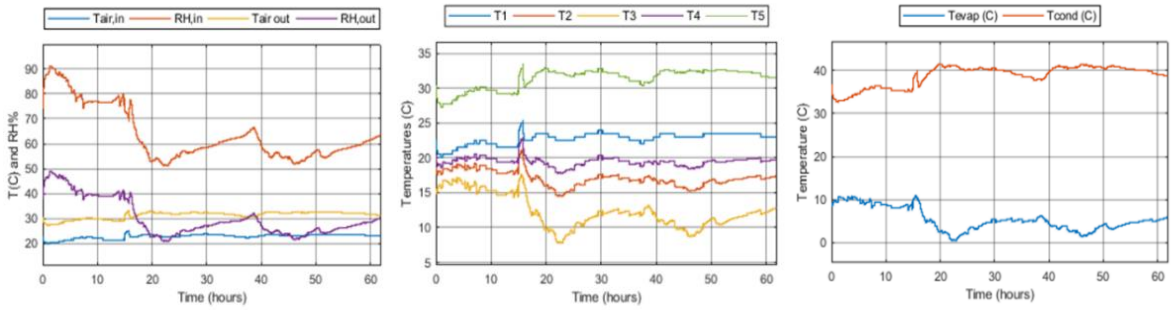

Fig. 9. Simulation results of heat pump performance. Left the air temperature and relative humidity at inlet and outlet of the heat pump dryer. In the center the air temperature changes along the different components (see Fig. 7 for positions). Right the condensation and evaporation temperatures of the heat pump.

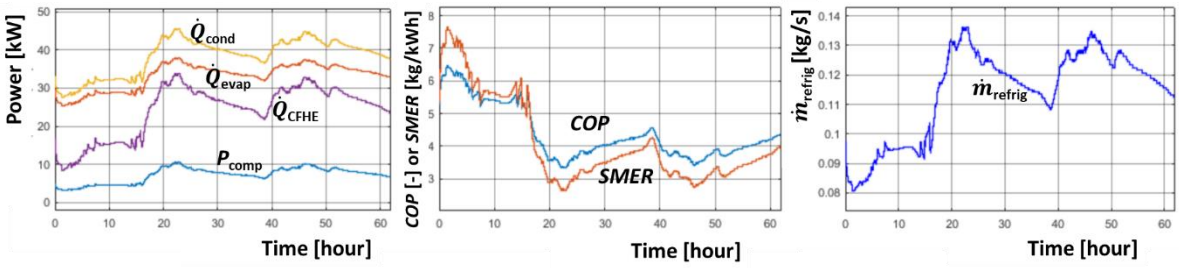

Fig. 10. Simulation results of heat pump performance. Left the heat exchanged in the different components. In the center the *COP* and *SMER* of the system. Right the required mass flow of refrigerant as a function of time.

7. Conclusions

In this study a Simulink model has been developed for the drying process of flower bulbs which includes a vapor compression heat pump assisted with a cross flow heat exchanger for heat recovery. The model results have been validated making use of experimental data collected at a flower bulb company. The main conclusions of this study are as follows:

- The drying process of the flower bulbs distinguishes two regimes: first the unbounded water is evaporated from the surface of the bulbs at a constant rate after which the water from the core of the bulbs starts to be removed and the moisture removal rate linearly decreases until an equilibrium is attained.
- Approaching the flower bulb boxes as packed beds of spherical shaped bulbs with void fraction of 19.6% and average diameter of 4.1 cm gives results comparable to the experimental values for what concerns the drying rate.

- To prevent too high temperatures of the air entering the flow bulb boxes, compressor speed control is required. The expected load conditions are in the range 60 to 100%.
- In the first 15 hours of operation the *COP* of the heat pump reaches values in the range of 6. However, improvement of the design of the condenser and evaporator is possible since, in the present design, the temperature driving forces across these heat exchangers are quite large.
- During the first 15 hours of operation the heat pump removes around 25 kg of moisture per flower bulb box. This is around 3% of the total weight per box.
- During the first 15 hours of operation the heat pump extracts 6 kg of moisture per kWh of energy consumed.
- While a conventional fossil fuel driven drying system consumes 350 kWh per day, the proposed heat pump dryer consumes 170 kWh renewable electricity per day.
- Implementation of heat pumps for drying purposes in the agriculture sector results in energy savings combined with improved product quality while burning of fossil fuels is prevented.

Acknowledgements

The authors would like to thank Niels Kreuk BV and Gebr. Boon Hem BV for facilitating the experimental work and Wagenaar Koeltechniek for delivering the data-collecting equipment.

References

[1] Agrawal SG, Methekar RN, 2017. Mathematical model for heat and mass transfer during convective drying of pumpkin. Food and Bioproducts Processing **101**: 68-73.
[2] Alnaimat F, Klausner JF, Mei R, 2011. Transient analysis of direct contact evaporation and condensation within packed beds. International Journal of Heat and Mass Transfer **54-15-16**: 3381-3393.
[3] Conway JH, Sloane NJA, 1999. Sphere packings, lattices and groups. 3rd Edition. Springer-Verlag New York.
[4] ECN & CBS, 2017. *Nationale energieverkenning*. ECN-O-14-036; The Netherlands.
[5] Hand R, Ernens B, 2014. Voorstudie: duurzaam drogen van bloembollen middels een droogsysteem met zuigende ventilatoren en actieve ontvochtiging. Report 13985.
[6] Kalbasi M, 2003. Heat and moisture transfer model for onion drying. Drying Technology **21-8**: 1575-1584.
[7] Kemp IC, 2014. Fundamentals of energy analysis of dryers. *Modern Drying Technology* **4-4**:1–45.
[8] Li Y, Klausner J, Mei R, Knight J, 2006. Direct contact condensation in packed beds. International Journal of Heat and Mass Transfer **49-25-26**: 4751-4761.
[9] Madamba PS, Driscoll RH, Buckle KA, 2007. Predicting the sorption behaviour of garlic slices. Drying Technology **12-3**: 669-683.
[10]Mills AF, 1999. Basic heat & mass transfer. 2nd Edition. Prentice Hall, New Jersey.
[11]Minea V, 2016. Advances in heat pump-assisted drying technology. CRC Press, New York.
[12]Mujumbar, AS, 2014. Handbook of industrial drying. 4th Edition. CRC Press, New York.
[13]Ogulata RT, Doba F, 1998. Experiments and entropy generation minimization analysis of a cross-flow heat exchanger. International Journal of Heat and Mass Transfer **41-2**: 373-381.
[14]Rockland LB, Beuchat LR, 1987. Water activity: theory and applications to food. 2nd Edition. Marcel Dekker, New York.
[15]Tzempelikos DA, Mitrakos D, Vouros AP, Bardakas AV, Filios AE, Margaris DP, 2015. Numerical modeling of heat and mass transfer during convective drying of cylindrical quince slices. Journal of Food Engineering **156**: 10-21.
[16]van Hiele T, Koster GJ, van Male J, Nunes EL, 1986. Handboek voor de koudetechniek. Uitgeverij P.C. Noordervliet BV, Zeist. The Netherlands.
[17]Wagenaar S, 2019. Feasibility study of a heat pump assisted flower bulb drying system. MSc thesis in Mechanical Engineering. Delft University of Technology.
[18]Wildschut J, 2018. Energiemonitor van de Nederlandse Bloembollensector 2016. Bleiswijk: Wageningen University & Research, BU Glastuinbouw - Bloembollen. 38 p. (Report Wageningen Plant Research; no. WPR-816).
[19]Wildschut J., Dijkema M, van der Lans A, 2013. Ventilatie, Ademhaling en CO_2-schadedrempels. Praktijkonderzoek Plant & Omgeving B.V. Report PPO nr. 32 36156400.